

RESEARCH ARTICLE

Activation response and functional connectivity change in rat cortex after bilateral transcranial direct current stimulation—An exploratory study

Julia Boonzaier¹ | Milou Straathof¹ | Dirk Jan Ardesch² | Annette van der Toorn¹ | Gerard van Vliet¹ | Caroline L. van Heijningen¹ | Willem M. Otte^{1,3} | Rick M. Dijkhuizen¹ 

¹Biomedical Magnetic Resonance Imaging and Spectroscopy Group, Center for Image Sciences, University Medical Center Utrecht and Utrecht University, Utrecht, The Netherlands

²Connectome Lab, Department of Complex Trait Genetics, Center for Neurogenomics and Cognitive Research, Vrije Universiteit Amsterdam, Amsterdam Neuroscience, Amsterdam, The Netherlands

³Department of Pediatric Neurology, UMC Utrecht Brain Center, University Medical Center Utrecht and Utrecht University, Utrecht, The Netherlands

Correspondence

Rick M. Dijkhuizen, Biomedical Magnetic Resonance Imaging and Spectroscopy Group, Center for Image Sciences, University Medical Center Utrecht, Yalelaan 2, 3584 CM Utrecht, The Netherlands. Email: r.m.dijkhuizen@umcutrecht.nl

Funding information

Netherlands Organization for Scientific Research [VICI 016.130.662]

Edited by Sandra Chanruad and Cristina Ghiani. Reviewed by Stephane Perrey, Maria Concetta Pellicciari, and Kai-Hsiang Chuang.

Julia Boonzaier, Milou Straathof and Dirk Jan Ardesch should be considered joint first author.

This is an open access article under the terms of the Creative Commons Attribution-NonCommercial-NoDerivs License, which permits use and distribution in any medium, provided the original work is properly cited, the use is non-commercial and no modifications or adaptations are made.

© 2021 The Authors. *Journal of Neuroscience Research* published by Wiley Periodicals LLC.



Abstract

Transcranial direct current stimulation (tDCS) is a noninvasive brain stimulation technique implicated as a promising adjunct therapy to improve motor function through the neuromodulation of brain networks. Particularly bilateral tDCS, which affects both hemispheres, may yield stronger effects on motor learning than unilateral stimulation. Therefore, the aim of this exploratory study was to develop an experimental model for simultaneous magnetic resonance imaging (MRI) and bilateral tDCS in rats, to measure instant and resultant effects of tDCS on network activity and connectivity. Naïve, male Sprague-Dawley rats were divided into a tDCS ($n = 7$) and sham stimulation group ($n = 6$). Functional MRI data were collected during concurrent bilateral tDCS over the sensorimotor cortex, while resting-state functional MRI and perfusion MRI were acquired directly before and after stimulation. Bilateral tDCS induced a hemodynamic activation response, reflected by a bilateral increase in blood oxygenation level-dependent signal in different cortical areas, including the sensorimotor regions. Resting-state functional connectivity within the cortical sensorimotor network decreased after a first stimulation session but increased after a second session, suggesting an interaction between multiple tDCS sessions. Perfusion MRI revealed no significant changes in cerebral blood flow after tDCS. Our exploratory study demonstrates successful application of an MRI-compatible bilateral tDCS setup in an animal model. Our results indicate that bilateral tDCS can locally modulate neuronal activity and connectivity, which may underlie its therapeutic potential.

KEYWORDS

animal, magnetic resonance imaging, models, resting-state functional connectivity, transcranial direct current stimulation

1 | INTRODUCTION

Transcranial direct current stimulation (tDCS) is a noninvasive neuro-modulation technique implicated as a promising therapeutic strategy to modify neuronal plasticity, for example, to improve motor function (Bai et al., 2019). Through the transcranial application of weak direct currents, changes in intracortical excitability can be elicited due to subthreshold modulation of neuronal membrane potentials (Nitsche et al., 2003; Stagg & Nitsche, 2011; Woods et al., 2016). The extent of these modulations largely depends on current intensity and electrode montage (unilateral vs. bilateral), which can alter cortical excitability in a polarity-specific manner (Jackson et al., 2016). Anodal tDCS has been assumed to augment neuronal excitability while cathodal tDCS would diminish it (Nitsche et al., 2003; Nitsche & Paulus, 2000). With regard to motor function, it has been suggested that bilateral tDCS, with the anode over the nondominant motor cortex and the cathode over the dominant motor cortex, may yield stronger effects on motor learning as compared to unilateral stimulation (Halakoo et al., 2020; Vines et al., 2008). As a consequence, there is a particular interest to use bilateral stimulation as an adjuvant therapy during physical rehabilitation of stroke patients with motor deficits (Di Lazzaro et al., 2014; Di Pino et al., 2014). Hypothetically, bilateral motor cortex modulation may particularly help to restore the interhemispheric imbalance associated with motor dysfunction, through anodal-mediated facilitation of neuronal activity in the damaged hemisphere while at the same time reducing neuronal (over)excitability of the unaffected hemisphere underneath the cathode (Sehm et al., 2013). Nevertheless, the effects of bilateral tDCS on brain activity and function remain incompletely characterized.

Direct and delayed effects of tDCS at a whole-brain network level may be effectively measured with *in vivo* neuroimaging tools, such as optical spectroscopy/imaging (Khan, 2013; Merzagora et al., 2010; Muthalib et al., 2018) and magnetic resonance imaging (MRI) (Takano et al., 2011). Moreover, with functional MRI, cerebral blood flow (CBF), neuronal activation responses, and functional connectivity can be measured concurrently in a single session. Several studies have reported tDCS-induced changes in CBF and blood oxygenation level-dependent (BOLD) signal. These CBF and BOLD changes have been found in widespread cortical networks during motor tasks, with cathodal tDCS inducing the largest changes (Baudewig et al., 2001; Lang et al., 2005). Anodal tDCS, in contrast, seems to only generate modest changes after stimulation periods of varying duration (Baudewig et al., 2001; Jang et al., 2009; Lang et al., 2005). Surprisingly, the changes in CBF and BOLD signals are observed on a global scale, although the polarizing effects of tDCS are generally thought to be restricted to the cortical area under the electrodes (Stagg & Nitsche, 2011). Several studies have also demonstrated that tDCS can modulate resting-state functional connectivity across the brain (Amadi et al., 2014; Peña-Gómez et al., 2012; Polanía, Nitsche, et al., 2011; Polanía, Paulus, et al., 2011; Sehm et al., 2012). However, variable patterns of stimulation-induced changes have been reported.

Significance

Accumulating evidence supports the therapeutic potential of transcranial direct current stimulation (tDCS) in brain disorders, however tDCS-induced effects on functional brain networks remain unclarified. Experimental animal models can be fundamental to unraveling tDCS-induced effects. In this exploratory study we applied *in vivo* functional magnetic resonance imaging of neural activity and connectivity during bilateral tDCS of the sensorimotor cortex in rats, similar to approaches that showed manipulation of motor function in humans. We found that bilateral tDCS affects signals and signaling within and across the sensorimotor network, which may underlie its neuromodulatory potential.

Therefore, the main purpose of this exploratory study was to develop and apply an experimental *in vivo* setting for MRI during tDCS (in rats) to measure instant and resultant effects of cortical stimulation on whole-brain network status. This could aid in the elucidation of neuromodulatory actions of tDCS. We hypothesized that bilateral tDCS of the sensorimotor cortex induces a polarity-specific direct cortical activation response and, as an after-effect, polarity-specific modulation of functional connectivity within the sensorimotor cortical network.

2 | MATERIALS AND METHODS

All experiments were approved by the Animal Ethics Committee of the University Medical Center Utrecht, The Netherlands (DEC 2014.I.10.082), and were conducted in agreement with Dutch laws ("Wet op de Dierproeven," 1996) and European regulations (Guideline 86/609/EEC).

2.1 | Animals

Thirteen naïve, adult male Sprague-Dawley rats (9–10 weeks old; 385 ± 23 g (mean \pm SD) body weight; Charles River Laboratories, Sulzfeld, Germany) were group-housed under controlled environmental conditions (12-hr light/dark cycle, temperature 20–24°C, 45%–65% humidity). They were housed with a Perspex tube and tissue paper as cage enrichment, and had *ad libitum* access to food and water. Animals underwent surgery for placement of tDCS cannulas (see Figure 1a, experimental setup) after at least 7 days of acclimatization in the animal facility. After the surgical procedure, animals were housed solitarily, in flat-roof cages (with only tissue paper as enrichment) to prevent removal of the Perspex cannulas on their skulls. Rats were divided into a tDCS ($n = 7$) or sham stimulation

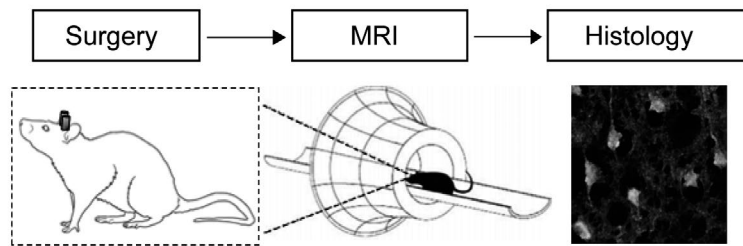
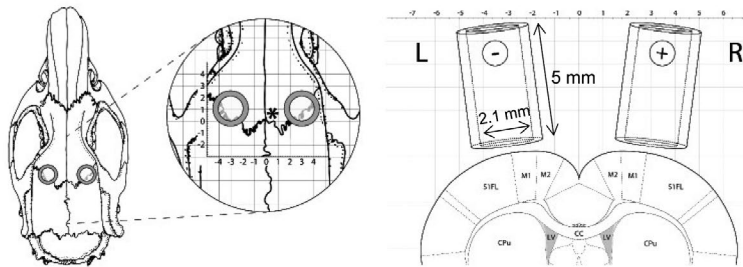
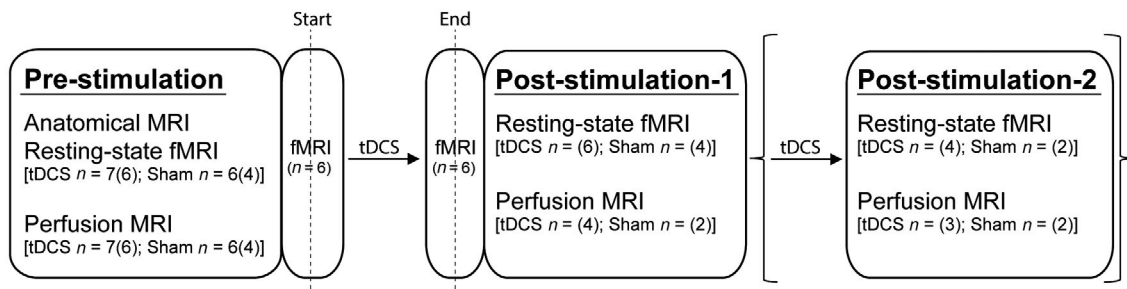
(a) Experimental setup**(b) Cannula placement and design****(c) MR imaging and stimulation protocol**

FIGURE 1 Bilateral transcranial direct current stimulation (tDCS) setup and magnetic resonance imaging (MRI) protocol. (a) Experimental design. One week before bilateral tDCS, cannulas were epicranially fixed to the skull. Animals received either one or two 15-min tDCS sessions while inside the MRI scanner. Following MRI, animals were perfusion-fixed and their brains were extracted for histological Fluoro-Jade B staining. (b, left view) Axial view of the rat skull indicating the positioning of the tDCS cannulas with respect to bregma (indicated by asterisk). Scale bars are in mm. (b, right view) Coronal rat brain slice showing the underlying cortical and subcortical regions underneath the stimulation cannulas (M1, M2, S1FL). The left tube (L) was used for the cathodal electrode and the right tube (R) was used for the anodal electrode, resulting in cathodal stimulation of the left sensorimotor cortex and anodal stimulation of the right sensorimotor cortex. (c) Anatomical MRI, resting-state functional MRI (rs-fMRI), and perfusion MRI were executed before the first stimulation session (15 min bilateral tDCS at 200 μ A). In order to assess the direct effect of stimulation, fMRI was run from approximately 2 min before to 2 min after the onset of stimulation, as well as from approximately 2 min before to 2 min after the end of stimulation in the tDCS group. After the first stimulation, rs-fMRI and perfusion MRI were acquired again. In a subset of animals, a second round of stimulation and subsequent rs-fMRI and perfusion MRI (indicated by parentheses) were executed. Prestimulation MRI started off with seven animals in the tDCS group and six animals in the sham group. Animal numbers specified between the round brackets, indicate the final number of animals used in each MRI analysis. CC, corpus callosum; CPu, caudate putamen; L, left; LV, lateral ventricle; M1, primary motor cortex, M2, secondary motor cortex; R, right; S1FL, forelimb region of the primary somatosensory cortex

group ($n = 6$). Sham stimulation animals underwent the same procedures as the tDCS group, but they did not receive any stimulation. Animal welfare was monitored by means of visual inspection and weighing every other day after surgery. Seven or 8 days after surgery, the animals were subjected to MRI and tDCS. Directly or 1 week after MRI acquisition, the animals were euthanized and perfusion-fixed.

2.2 | tDCS**2.2.1 | Surgical placement of bilateral, epicranial cannulas**

Animals were anesthetized with a mixture of O_2 /air (4:1) and isoflurane (5% induction). They were intubated, connected to a

mechanical ventilator (TOPO, Kent Scientific, Torrington, CT, USA), and positioned in a stereotaxic frame. Subcutaneous analgesia, 5 mg/kg Carprofen, was administered preoperatively for all rats. During the surgical procedure, isoflurane was maintained at 2.5%, and the body temperature of the animals was monitored and maintained at $37 \pm 0.5^\circ\text{C}$ with a circulating water heating mat. The scalp was shaved and disinfected, and a midline incision was made from the rostral eye level to the mid-ear level. The periosteum was cut and scraped to the edges of the skull and thoroughly wiped off. Two custom-made, cylindrical, Perspex cannulas (height 5.0 mm, outer/inner diameters 3.0/2.1 mm) were lowered onto the skull using a compass connected to the stereotaxic frame for precise positioning (Figure 1b). The cannulas were positioned bilaterally over the sensorimotor cortex, which included the primary (M1) and secondary (M2) motor cortices and the forelimb region of the somatosensory cortex (S1FL) (1.0 mm anterior to bregma and 3.0 mm lateral from the midline). A nontoxic, glass ionomer cement (Ketac Cem Plus Automix, 3M ESPE, Delft, the Netherlands) was applied on the skull and around the cannulas to keep them in place. Once the cement hardened, the skin was sutured around the cannulas, and two Perspex caps were placed onto the cannulas to prevent dust or bedding material from obstructing the stimulation area. A drop of Lidocaine (100 mg/ml spray, AstraZeneca B.V., Zoetermeer) was added to the wound for additional local analgesia. After surgery, the rats recovered from anesthesia in a preheated cage before being placed back solitarily in their home cages.

2.2.2 | MRI-compatible tDCS

The MRI-compatible tDCS setup consisted of a custom-built direct current stimulator, connected to two platinum wires entering the magnet bore. The ends of the wires were led through two Perspex caps placed onto the cannulas. Before MRI acquisition and tDCS, the cannulas were filled with agarose gel (1.5%, prepared in a phosphate-buffered solution). The anode was connected to the cannula over the right hemisphere while the cathode was connected to the cannula over the left hemisphere in all animals (Figure 1b). A tDCS session consisted of 15-min stimulation inside the MRI scanner, at a current intensity of 200 μA (anodal over the right sensorimotor cortex and cathodal over the left sensorimotor cortex). With a single electrode contact area of 3.5 mm², this resulted in a current density of 57.1 A/m² and a charge density of $51.4 \times 10^3 \text{ C/m}^2$ at the scalp. These stimulation parameters were assumed to be safe as they did not cause any adverse effects in similar studies (Liebetanz et al., 2006, 2009). To avoid stimulation break effects, the current was automatically ramped up and down for 10 s at the onset and offset of stimulation (Bindman et al., 1964).

2.3 | *In vivo* MRI

2.3.1 | Anesthesia and physiological monitoring

Shortly before *in vivo* MRI, animals were endotracheally intubated for mechanical ventilation with 2% isoflurane in O₂/air (4:1). During MRI

acquisition the respiration rate and end-tidal CO₂ were closely monitored with a capnograph (Multinex 4200, Datascope Corporation, Paramus, NJ, USA). Heart rate and blood oxygen saturation were monitored with a pulse oximeter (Nonin 8600V, Nonin Medical Inc., Plymouth, MN, USA), and body temperature was maintained at $37.0 \pm 1.0^\circ\text{C}$ using a feedback mechanism with a warm water circuit. Fifteen minutes prior to functional MRI acquisition, the isoflurane percentage was lowered to 1.5% to reduce anesthetic effects on subsequent functional MRI scans.

2.3.2 | Imaging protocol and timeline

For each rat, the scanning protocol started with an anatomical scan, followed by prestimulation measurements of resting-state functional connectivity with resting-state fMRI, and CBF with arterial spin labeling (ASL) (tDCS group: $n = 7$; sham stimulation: $n = 6$) (Figure 1c). The rats then underwent a first period of tDCS ($n = 7$) or sham stimulation ($n = 6$), followed by poststimulation-1 measurements with resting-state fMRI and ASL to assess the acute after-effects of tDCS. In addition, two short (5 min) fMRI acquisitions were performed at the start and end of the first tDCS period, respectively, to assess the activation response during and directly after stimulation (tDCS group ($n = 7$)). To limit the fMRI data file size, we discontinued scanning during the ca. 10 min of tDCS in between. In a subset of rats (tDCS group: $n = 4$; sham stimulation group: $n = 4$), a second 15-min tDCS session was performed (without simultaneous fMRI, due to technical reasons), followed by a poststimulation-2 measurement with resting-state fMRI and ASL, to evaluate whether a second stimulation would have similar or dissimilar effects. See the Supporting Information for the image acquisition details.

2.4 | Data processing

Image processing was performed using MATLAB (MATLAB R2016a, The MathWorks Inc., Natick, MA, 2016) and FSL v5.0.9 (Jenkinson et al., 2012), unless otherwise stated. See the Supporting Information for the preprocessing steps that were followed for each image acquisition.

2.4.1 | Image registration and regions of interest

Images were registered to a high-resolution template to enable the selection of regions of interest (ROIs) from the Paxinos and Watson atlas (2005). As ROIs, the left and right sensorimotor cortical network were included, consisting of the primary and secondary motor cortices (M1 and M2), primary somatosensory cortex (S1FL and S1HL for forelimb and hind limb regions, respectively) and the secondary somatosensory cortex (S2). In addition, as a control region outside the tDCS-targeted area, we selected two regions from the visual cortex, consisting of the left and right primary and secondary visual cortices (V1 and V2). Analyses were

performed on these sensorimotor and visual cortices, as well as on the individual ROIs, unless otherwise stated. For analyses of individual ROIs, only regions with sufficient assurance of spatial alignment were included (i.e., with more than eight voxels in individual fMRI and ASL image space), which resulted in the exclusion of V1 (left and right) as an individual ROI.

2.5 | Histology

During perfusion fixation, animals were flushed with a cold saline solution for 5 min, followed by the infusion of 4% paraformaldehyde in a phosphate-buffered solution for 20 min. Brains were extracted and kept in 4% paraformaldehyde for 24 hr, followed by storage in 40% ethanol for 24 hr, and finally in 70% ethanol until embedding in paraffin. Using a microtome, brains embedded in paraffin were sectioned at 8 μ m thickness at 2.5, 1.0, and -0.5 mm anterior to bregma, and stained with Fluoro-Jade B for the detection of degenerating neurons (Schmued et al., 2005). See the Supporting Information for the staining protocol. To validate our Fluoro-Jade B procedure, we used poststroke mouse brain tissue as a positive control to show stroke-induced neurodegeneration.

2.6 | Statistical analyses

Statistical analyses were performed in R (3.2.3) and Rstudio (R Core Team, 2014). For analysis of fMRI data obtained during and directly after tDCS, we performed the following comparisons with a Wilcoxon paired signed rank test, for the left and right sensorimotor and visual cortices: (a) mean BOLD signal intensities of the prestimulation baseline (first 60 s of first fMRI session) versus the mean BOLD signal intensities during stimulation (last 60 s of the first fMRI session), (b) mean BOLD signal intensities during tDCS (first 60 s of the second fMRI session) versus the mean BOLD signal intensities after tDCS was stopped (last 60 s of second fMRI session) (Figure 1c). Results were considered statistically significant with a p value lower than 0.05 after correction for multiple testing with a false discovery rate (FDR) correction.

For resting-state fMRI and perfusion MRI, we calculated difference values for the first stimulation (stimulation-1: poststimulation-1 value minus prestimulation value) and the second stimulation (stimulation-2: poststimulation-2 value minus poststimulation-1 value) for each connection (resting-state fMRI analyses) or region (ASL) of interest. These comparisons were performed to investigate the independent effects of the first and second stimulations on functional connectivity and CBF.

We applied a linear mixed model (*nlme* package (Pinheiro et al., 2018)) with the factor group (tDCS or sham stimulation) as between-subject variable and the factor stimulation (stimulation-1 or stimulation-2) as within-subject variable. We corrected this model for multiple connections of interest measured in each rat. The model

was hierarchically structured with random intercepts and network connections nested within animals. Consequently, the linear mixed model includes all network connections into a single model. The output informs on statistical significance for the whole model, but does not provide statistical information for single connections. Results were considered statistically significant if the p value was lower than 0.05. See the Supporting Information for additional information regarding the linear mixed model.

3 | RESULTS

3.1 | Final group sizes

Visual inspection of the data following initial preprocessing steps led to the exclusion of three animals (tDCS group: $n = 1$; Sham group: $n = 2$) due to the presence of MR artifacts. This led to the following final group sizes for the fMRI and resting-state fMRI data: fMRI, $n = 6$ (tDCS group); resting-state fMRI prestimulation: $n = 6$ (tDCS group), $n = 4$ (sham group); poststimulation-1: $n = 6$ (tDCS group), $n = 4$ (sham group); and poststimulation-2: $n = 4$ (tDCS group), $n = 2$ (sham group).

Breathing difficulties due to mucus build-up in the intubation tube during MRI prevented the execution of the entire MRI protocol and/or a second tDCS session in some animals. Consequently, ASL measurements from four animals had to be discarded after stimulation-1 (two from both groups) and stimulation-2 (one from tDCS group), respectively. This led to the following final group sizes for the ASL data: prestimulation: $n = 6$ (tDCS group), $n = 4$ (sham group); poststimulation-1: $n = 4$ (tDCS group), $n = 2$ (sham group); and poststimulation-2: $n = 3$ (tDCS group), $n = 2$ (sham group).

3.2 | Immediate effects of bilateral tDCS on BOLD signal

Increases in BOLD signal following bilateral tDCS were evident in frontal brain regions. This was also the case in or near strongly perfused territories, such as sinuses and ventricles (Figure 2a).

Within 1 min after onset of tDCS, the BOLD signal increased with $0.68 \pm 0.84\%$ (mean difference \pm SD from baseline; $p = 0.13$, FDR-corrected) in the sensorimotor cortex underneath the cathode (left) (Figure 2b). BOLD signal changes in the sensorimotor cortex underneath the anode (right) were smaller ($0.27 \pm 0.30\%$ from baseline; $p = 0.13$, FDR-corrected). Most animals showed an increase in BOLD signal intensities in the left and right sensorimotor cortex during tDCS stimulation, except for one animal in the left hemispheric analyses and two animals in the right hemispheric analyses. However, there was no statistically significant difference between the mean BOLD signal intensities during baseline and stimulation in those areas. This pattern was also detected in the individual sensorimotor regions (see Figure S1).

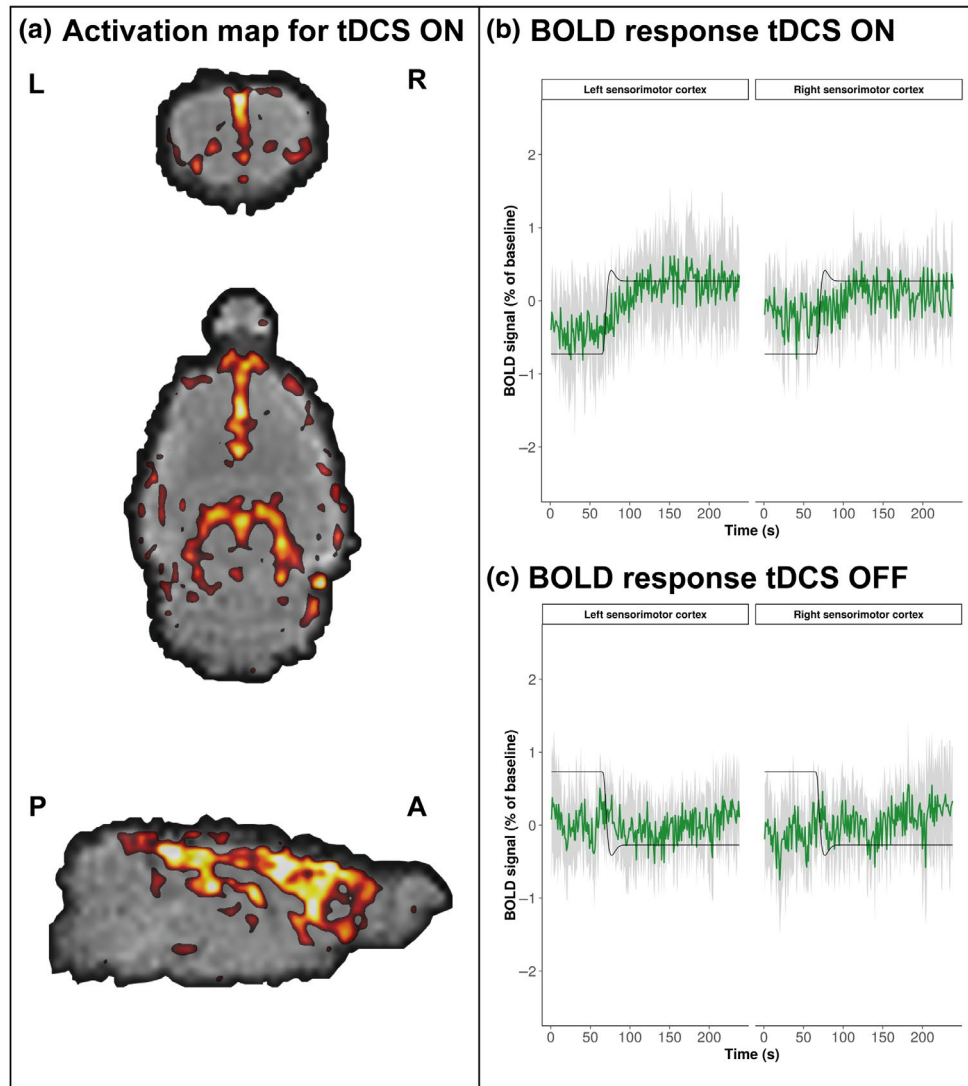


FIGURE 2 Blood oxygenation level-dependent (BOLD) response to bilateral transcranial direct current stimulation (tDCS). (a) Activation maps, calculated from a generalized linear model (GLM), showing areas with a statistically significant BOLD response to bilateral tDCS (first fMRI session), overlaid on coronal (top), axial (middle), and sagittal (bottom) echo-planar fMRI images of the rat brain. (b) BOLD signal time-course during the first fMRI session when tDCS was switched on, and (c) BOLD signal time-course during the second fMRI session when tDCS was switched off, in the left and right sensorimotor cortices, underneath the cathode and anode, respectively. The modeled BOLD response is overlaid on each graph as a black line. A, anterior; L, left; P, posterior; R, right [Color figure can be viewed at wileyonlinelibrary.com]

For all ROIs, when tDCS was switched off, the BOLD signal remained at the same level within the first 2 min. Accordingly, no significant differences were measured between the BOLD signals during and after stimulation in the second fMRI session (Figures 2c, S1 and S2).

Physiological conditions during simultaneous tDCS and fMRI were stable (see Figure S3).

3.3 | After-effects of bilateral tDCS on CBF

Bilateral tDCS, following the first and second stimulation session, did not induce any statistically significant CBF changes in the left or right sensorimotor cortex (Figures 3 and S4).

3.4 | After-effects of bilateral tDCS on resting-state functional connectivity

A network plot (Figure 4) shows the stimulation-induced changes in functional connectivity after stimulation-1 and stimulation-2. In the left sensorimotor cortex, underneath the cathode, we found a significant interaction effect between group and time ($\beta = 0.169$, 95% confidence interval = 0.0596–0.277, $t(\text{degrees-of-freedom: } 58) = 3.10$, $p = 0.0030$). Functional connectivity decreased after the first tDCS session and increased after the second stimulation session in the tDCS group, whereas the opposite pattern was apparent in the sham group. Also see Figure S5 for further information.

For the right sensorimotor cortex, underneath the anode, a significant time effect ($\beta = 0.134$, 95% confidence

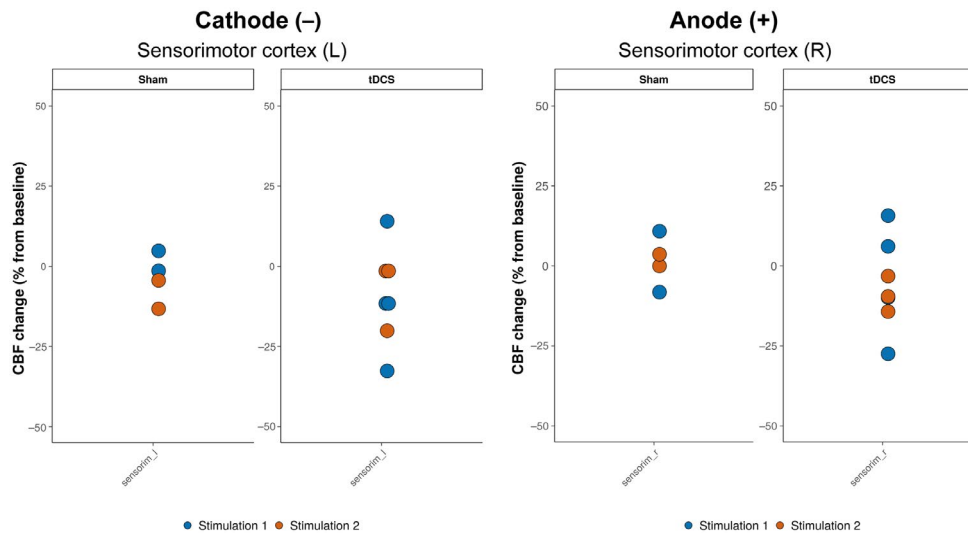


FIGURE 3 Cerebral blood flow (CBF) change after bilateral transcranial direct current stimulation (tDCS). CBF changes after the first and second stimulation session (sham or tDCS) in the left and right sensorimotor cortex, that is, underneath the cathode and anode, respectively. The colored dots represent individual data points. L, left; R, right [Color figure can be viewed at wileyonlinelibrary.com]

interval = 0.0499–0.217, $t(58) = 3.19$, $p = 0.0023$) was found. The first stimulation session appeared to slightly decrease functional connectivity, but the second stimulation session was followed by a noticeable increase in functional connectivity. However, these effects were present in both the tDCS and sham groups.

We did not detect significant effects of bilateral tDCS on functional connectivity between the visual cortical regions. Nor did we detect tDCS-induced changes in interhemispheric functional connectivity (Figure S5b).

3.5 | Histological effects of bilateral tDCS

To test whether our bilateral tDCS approach induced histological damage, we applied postmortem brain tissue staining with Fluoro-Jade B for all animals after tDCS or sham stimulation. No evidence of neurodegeneration was found in the tDCS or sham groups (Figure 5). Clear neuronal damage was detected with Fluoro-Jade B when using positive control tissue, that is, poststroke mouse brain (data not shown).

4 | DISCUSSION

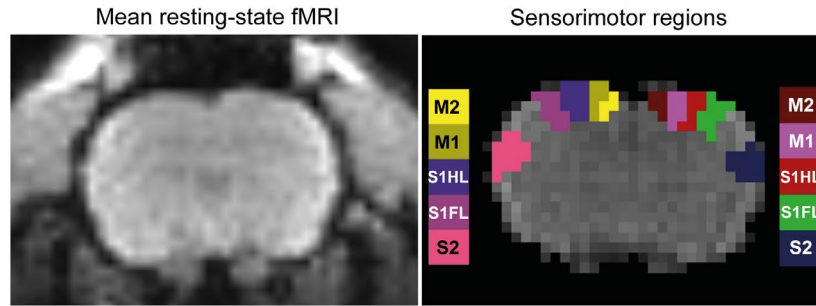
We assessed the neural response to bilateral tDCS in a rat model using functional MRI. Simultaneous bilateral tDCS and fMRI revealed increases in BOLD signal intensity in cortical brain regions, and in other strongly perfused regions. BOLD signal responses were also apparent in the sensorimotor cortex underneath the electrodes. Resting-state fMRI experiments showed that the first tDCS session led to a decrease in intrahemispheric functional connectivity within sensorimotor cortical regions, whereas functional connectivity increased after a second stimulation session. These functional

connectivity changes were most pronounced underneath the cathode. CBF, as measured with ASL, remained relatively stable after tDCS.

4.1 | Hemodynamic changes in response to tDCS

Previous studies in humans (Antal et al., 2011; Muthalib et al., 2018) and rats (Takano et al., 2011) have reported a BOLD activation response to tDCS, which was particularly noticeable in regions underneath the stimulation sites. Our results are in line with the findings in those studies. The observed increases in BOLD signal during bilateral tDCS may reflect direct effects of tDCS on cortical vessels, or a hemodynamic response to neuronal activation through neurovascular coupling (Stagg & Johansen-Berg, 2013). A direct effect of tDCS on smooth muscle cells in the vessel walls could explain colocalization of BOLD signal increase with large vessels (Wachter et al., 2011). However, tDCS-induced BOLD signal changes were also observed in brain areas that extended beyond the direct stimulation sites, including the visual cortex. This indicates that the bilateral tDCS paradigm induced an activation of a large neuronal and/or vascular network, possibly through connectivity, supportive of its suggested neuromodulatory capacity. In addition, the electrodes were relatively large compared to the rat brain, which probably contributed to the widespread response. In contrast, BOLD signal changes might have also been directly caused by systemic interference or by the electrical currents that run through tissue between the electrodes, as has previously been observed in postmortem subjects (Antal et al., 2014). Although electrical field distortions in the magnetic field cannot be excluded as a potential cause, we deem it unlikely that the observed BOLD response is only due to a stimulation artifact, because BOLD signal changes were detected in areas remote from the stimulation site. Unfortunately, we did not include

(a) Representative resting-state fMRI images



(b) Functional connectivity changes

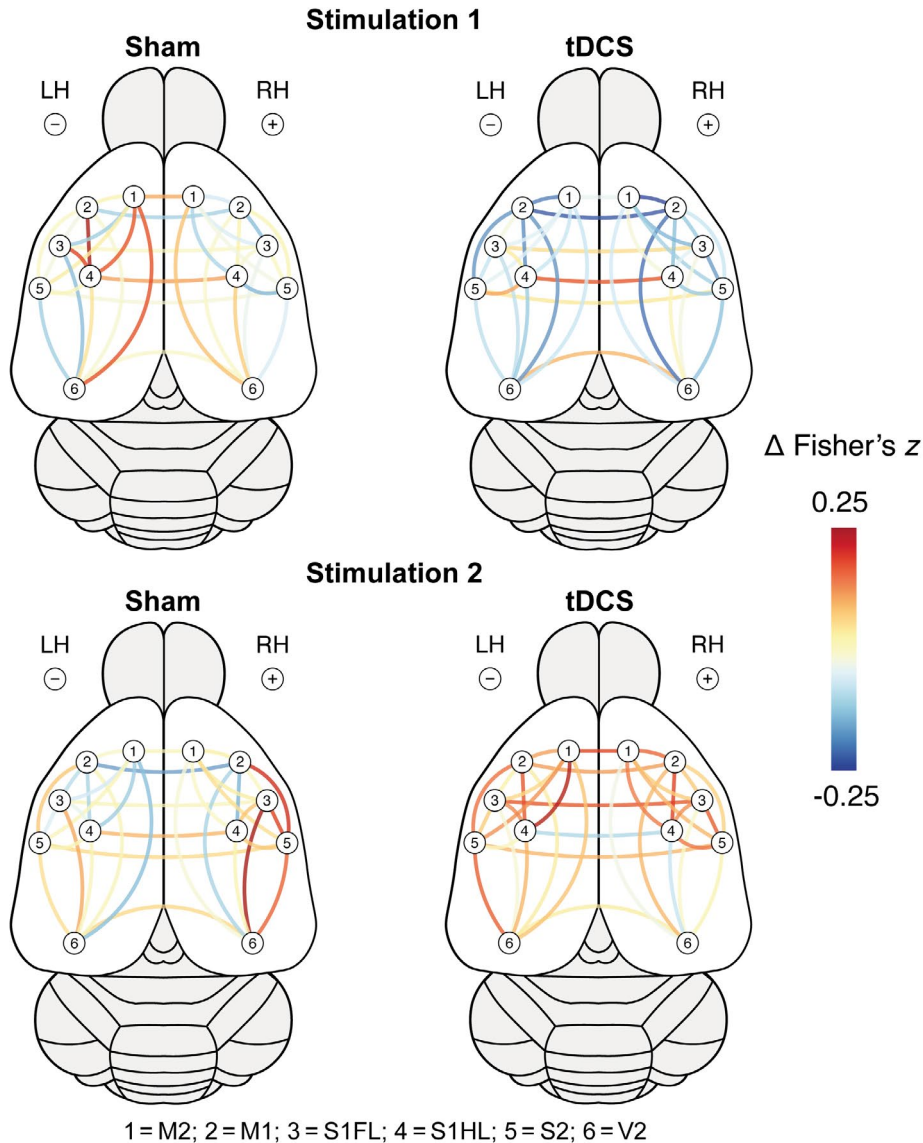


FIGURE 4 Changes in intra- and interhemispheric functional connectivity between cortical sensorimotor regions, following bilateral transcranial direct current stimulation (tDCS). (a) Representative mean resting-state fMRI (rs-fMRI) image of a coronal rat brain slice (left), and the regions of interest within the right (R) and left (L) sensorimotor cortex, overlaid on a rs-fMRI image. (b) Changes in intrahemispheric and interhemispheric functional connectivity (i.e., Fisher's z correlation) between regions of interest within the sensorimotor and visual cortices, following stimulation (tDCS or sham stimulation) session 1 and 2, represented by color-coded lines. LH, left hemisphere; M2, secondary motor cortex; M1, primary motor cortex; RH, right hemisphere; S2, secondary somatosensory cortex; S1FL, forelimb region of the primary somatosensory cortex; S1HL, hind limb region of the somatosensory cortex; V2, secondary visual cortex [Color figure can be viewed at wileyonlinelibrary.com]

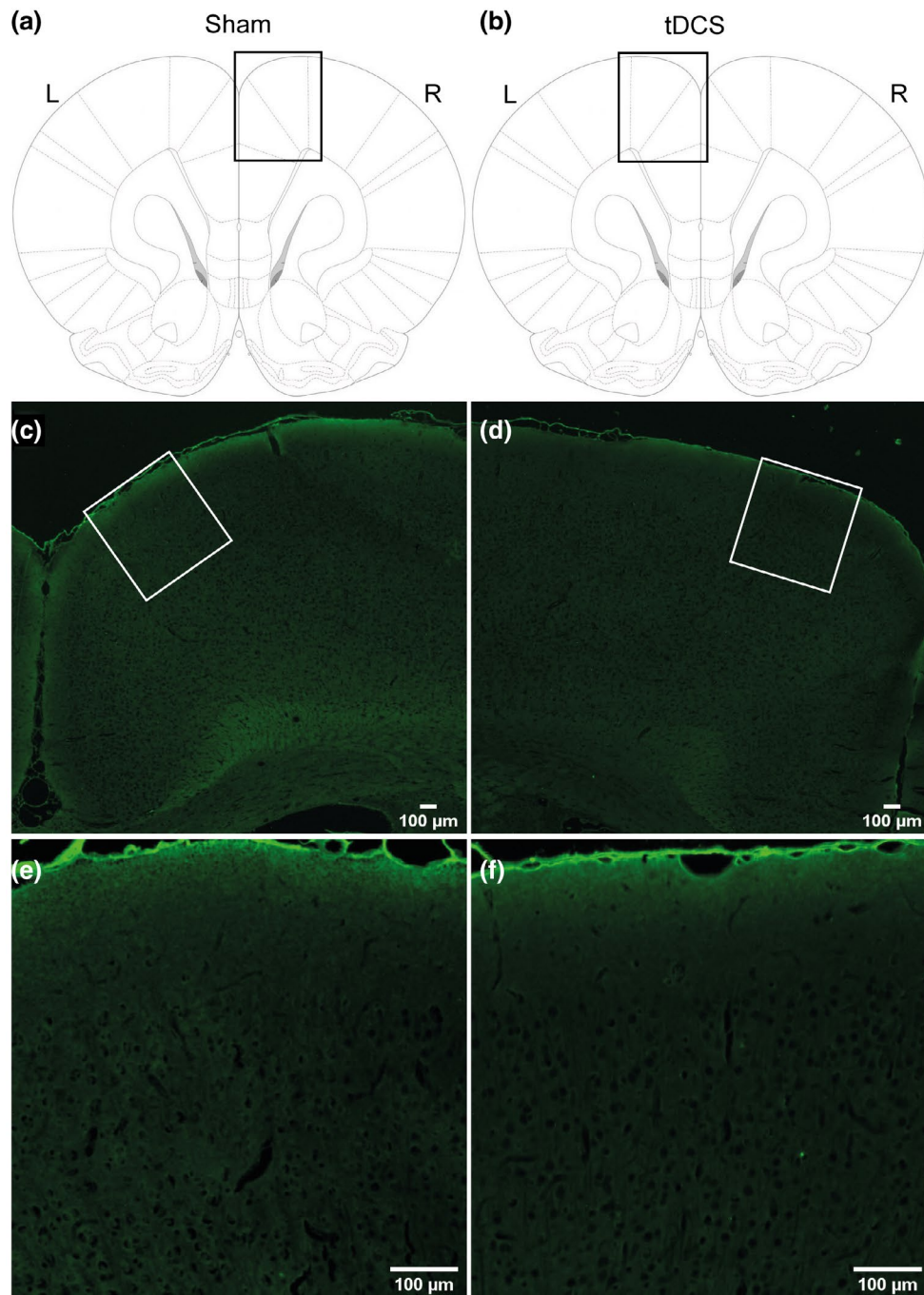


FIGURE 5 Fluoro-Jade B staining of rat brain after sham stimulation or transcranial direct current stimulation (tDCS). The top row (a,b) illustrates where a micrograph was made from a coronal rat brain slice. Middle and bottom row: 2.5× (c,d) and 10× magnified image (e,f), respectively. The absence of fluorescent signal illustrates the lack of neurodegeneration. Scale bar for all sections: 100 μm [Color figure can be viewed at wileyonlinelibrary.com]

measurements of the BOLD signal during sham stimulation to rule out possible neural effects of sham tDCS.

Although we detected a direct BOLD activation response to tDCS, we did not measure significant stimulation-induced after-effects on CBF. This appears to be in contrast with previous animal (Mielke et al., 2013; Wachter et al., 2011) and human (Lang et al., 2005; Zheng et al., 2011) imaging studies where polarity-specific changes in CBF have been observed after unilateral tDCS. However, in subjects that

received bilateral tDCS, similar to our study, no significant stimulation effects on CBF were measured when subjects were at rest (Paquette et al., 2011). Yet, when these subjects performed a motor task during bilateral stimulation, the change in CBF in M1 was found to be significantly lower on the cathodal than on the anodal side, as compared to sham stimulation (Paquette et al., 2011). This suggests that bilateral tDCS specifically modulated the task-induced neuronal activation in that study. Han and colleagues demonstrated with functional

near-infrared spectroscopy that a tDCS-induced increase in oxygenated-hemoglobin concentration—a measure related to regional CBF—decreased linearly after stimulation stopped (Han et al., 2014). In contrast, previous animal studies (Mielke et al., 2013; Wachter et al., 2011), using laser Doppler flowmetry, reported long-lasting (>30 min) polarity-specific changes in CBF after unilateral tDCS. In addition to variable effects of different stimulation paradigms, the sensitivity of methods to measure CBF may vary considerably. The ASL approach that we have used, which showed quite some variation in CBF baseline values, may not have been optimal for the measurement of subtle CBF changes.

4.2 | Resting-state functional connectivity after tDCS

We detected a significant interaction effect between group and time for the left sensorimotor cortex underneath the cathode. This indicated that the first and second stimulations had different effects in the tDCS and sham groups. This was not apparent for the right sensorimotor cortex. The left hemisphere of the tDCS group showed a decrease in functional connectivity after the first stimulation and an increase after the second stimulation. Thus, it seems like bilateral tDCS affects functional connectivity differently in each hemisphere, and possibly the anode enhanced the induced effects of the cathode.

The effects of the cathode on the left hemisphere functional connectivity may be related to a hyperpolarization phenomenon previously hypothesized by Amadi et al. (2014) and Polanía et al. (2012). They found an increase in the strength of local functional connections after cathodal tDCS in human studies. It was hypothesized that this increase in functional connectivity following cathodal tDCS is due to neuronal hyperpolarization. Hyperpolarizations would effectively reduce local neuronal noise, lead to an increase in signal-to-noise ratio, and increase neuronal synchronization within the stimulated area. However, bilateral tDCS studies have reported different responses. These include bihemispheric (Lindenberg et al., 2016) and unihemispheric (Sehm et al., 2012) polarity-specific changes in functional connectivity (increase after anodal and decrease after cathodal stimulation, respectively) and widespread bihemispheric changes in connectivity (Pellegrino et al., 2018; Polanía, Paulus, et al., 2011). These differences emphasize the need for systematic and thorough studies on the neurophysiological effects of tDCS. Such studies may help to improve standardization of translational experiments in animal models.

Although speculative, the observed increase in resting-state functional connectivity after the second stimulation session might be explained by a preconditioning effect. Since the effects of a single stimulation session may last for at least 1–2 hr (Bączyk & Jankowska, 2014; Liebetanz et al., 2006; Nitsche & Paulus, 2001), it is conceivable that the first stimulation session preconditioned the targeted networks, that is, lowered the threshold. As a result, the second stimulation session could have caused a reversed effect on resting-state functional connectivity. However, our sample size was small and further experiments are needed to confirm these specific findings.

4.3 | Histological effects of bilateral tDCS

The stimulation parameters (current intensity of 200 μ A, current density of 57.1 A/m², and charge density of 51.4×10^3 C/m²) used in this study did not lead to histological damage. This suggests that these stimulation parameters, in line with proposed safety settings reported by Liebetanz and colleagues (Liebetanz et al., 2006, 2009), are safe. Stimulation dosage is a critical aspect in the translation between animal and human tDCS studies. However, comparison of stimulation parameters may not be straightforward (Ling et al., 2016) and requires further computational and physiological validation.

4.4 | Study limitations

Our study, which is exploratory in nature, is limited by the small sample size, which was further affected by a number of technical issues that led to the dropout of some animals. Also, we did not measure the modulatory tDCS effects on cortical excitability, nor did we include electrophysiological measurements that could provide additional insights into the mechanism of action of bilateral tDCS. Prospective follow-up studies should also consider strategies that minimize possible confounding effects on the BOLD fMRI signal, such as lower anesthesia levels, correction for signal drift, and inclusion of signal from large vessels as a covariate in analyses.

4.5 | Conclusion

In conclusion, our exploratory study shows successful application of an MRI-compatible bilateral tDCS setup in an animal model. Our results demonstrate that bilateral tDCS over the sensorimotor cortex affects signals and signaling within and across the sensorimotor cortical network in the healthy rat brain. This includes modulation of neuronal activity and connectivity as measured with functional MRI. Further studies are needed to assess these effects under pathophysiological conditions, such as after stroke, where (bilateral) tDCS may contribute to functional recovery.

DECLARATION OF TRANSPARENCY

The authors, reviewers and editors affirm that in accordance to the policies set by the *Journal of Neuroscience Research*, this manuscript presents an accurate and transparent account of the study being reported and that all critical details describing the methods and results are present.

ACKNOWLEDGMENTS

The authors thank Caren van Kammen and Dr. Cora Nijboer for their help with the tissue staining, and Prof. Gilles van Luitelaar and Gerard van Oijen for their technical assistance with the development of our tDCS device.

CONFLICT OF INTEREST

The authors declare no competing interests.

AUTHOR CONTRIBUTIONS

Conceptualization, J.B., D.J.A., and R.M.D.; *Methodology*, J.B., D.J.A., G.v.V., A.v.d.T., and C.L.H.; *Project Administration*, D.J.A. and C.L.H.; *Investigation*, D.J.A., J.B., and M.S.; *Formal Analysis*, M.S., W.O., and J.B.; *Software*, A.v.d.T. and G.v.V.; *Resources*, R.M.D.; *Writing – Original Draft*, J.B. and M.S.; *Writing – Review & Editing*, R.M.D., W.O., A.v.d.T., M.S., D.J.A., and J.B.; *Visualization*, M.S., J.B., and D.J.A.; *Funding Acquisition*, R.M.D.; *Supervision*, R.M.D. and J.B.

PEER REVIEW

The peer review history for this article is available at <https://publons.com/publon/10.1002/jnr.24793>.

DATA AVAILABILITY STATEMENT

The data supporting the findings of this study are available from the corresponding author upon reasonable request.

ORCID

Rick M. Dijkhuizen  <https://orcid.org/0000-0002-4623-4078>

REFERENCES

- Amadi, U., Ilie, A., Johansen-Berg, H., & Stagg, C. J. (2014). Polarity-specific effects of motor transcranial direct current stimulation on fMRI resting state networks. *Neuroimage*, *88*, 155–161. <https://doi.org/10.1016/j.neuroimage.2013.11.037>
- Antal, A., Bikson, M., Datta, A., Lafon, B., Dechent, P., Parra, L. C., & Paulus, W. (2014). Imaging artifacts induced by electrical stimulation during conventional fMRI of the brain. *Neuroimage*, *85*, 1040–1047. <https://doi.org/10.1016/j.neuroimage.2012.10.026>
- Antal, A., Polania, R., Schmidt-Samoa, C., Dechent, P., & Paulus, W. (2011). Transcranial direct current stimulation over the primary motor cortex during fMRI. *Neuroimage*, *55*, 590–596. <https://doi.org/10.1016/j.neuroimage.2010.11.085>
- Bączyk, M., & Jankowska, E. (2014). Presynaptic actions of transcranial and local direct current stimulation in the red nucleus. *Journal of Physiology*, *19*, 4313–4328. <https://doi.org/10.1113/jphysiol.2014.276691>
- Bai, X., Guo, Z., He, L., Ren, L., McClure, M. A., & Mu, Q. (2019). Different therapeutic effects of transcranial direct current stimulation on upper and lower limb recovery of stroke patients with motor dysfunction: A meta-analysis. *Neural Plasticity*, *2019*, 1–13. <https://doi.org/10.1155/2019/1372138>
- Baudewig, J., Nitsche, M. A., Paulus, W., & Frahm, J. (2001). Regional modulation of BOLD MRI responses to human sensorimotor activation by transcranial direct current stimulation. *Magnetic Resonance in Medicine*, *45*, 196–201. [https://doi.org/10.1002/1522-2594\(200102\)45:2<196::AID-MRM1026>3.0.CO;2-1](https://doi.org/10.1002/1522-2594(200102)45:2<196::AID-MRM1026>3.0.CO;2-1)
- Bindman, L. J., Lippold, O. C. J., & Redfearn, J. W. T. (1964). The action of brief polarizing currents on the cerebral cortex of the rat (1) during current flow and (2) in the production of long-lasting after-effects. *Journal of Physiology*, *172*, 369–382. <https://doi.org/10.1113/jphysiol.1964.sp007425>
- Di Lazzaro, V., Dileone, M., Capone, F., Pellegrino, G., Ranieri, F., Musumeci, G., Florio, L., Di Pino, G., & Fregni, F. (2014). Immediate and late modulation of interhemispheric imbalance with bilateral transcranial direct current stimulation in acute stroke. *Brain Stimulation*, *7*, 841–848. <https://doi.org/10.1016/j.brs.2014.10.001>
- Di Pino, G., Pellegrino, G., Assenza, G., Capone, F., Ferreri, F., Formica, D., Ranieri, F., Tombini, M., Ziemann, U., Rothwell, J. C., & Di Lazzaro, V. (2014). Modulation of brain plasticity in stroke: A novel model for neurorehabilitation. *Nature Reviews. Neurology*, *10*, 597–608. <https://doi.org/10.1038/nrneurol.2014.162>
- Halakoo, S., Ehsani, F., Hosnian, M., Zoghi, M., & Jaberzadeh, S. (2020). The comparative effects of unilateral and bilateral transcranial direct current stimulation on motor learning and motor performance: A systematic review of literature and meta-analysis. *Journal of Clinical Neuroscience*, *72*, 8–14. <https://doi.org/10.1016/j.jocn.2019.12.022>
- Han, C.-H., Song, H., Kang, Y.-G., Kim, B.-M., & Im, C.-H. (2014). Hemodynamic responses in rat brain during transcranial direct current stimulation: A functional near-infrared spectroscopy study. *Biomedical Optics Express*, *5*, 1812–1821. <https://doi.org/10.1364/BOE.5.001812>
- Jackson, M. P., Rahman, A., Lafon, B., Kronberg, G., Ling, D., & Parra, L. C. B. M. (2016). Animal models of transcranial direct current stimulation: Methods and mechanisms. *Clinical Neurophysiology*, *127*, 3425–3454. <https://doi.org/10.1016/j.clinph.2016.08.016>
- Jang, S. H., Ahn, S. H., Byun, W. M., Kim, C. S., Lee, M. Y., & Kwon, Y. H. (2009). The effect of transcranial direct current stimulation on the cortical activation by motor task in the human brain: An fMRI study. *Neuroscience Letters*, *460*, 117–120. <https://doi.org/10.1016/j.neulet.2009.05.037>
- Jenkinson, M., Beckmann, C. F., Behrens, T. E. J., Woolrich, M. W., & Smith, S. M. (2012). FSL. *Neuroimage*, *62*, 782–790. <https://doi.org/10.1016/j.neuroimage.2011.09.015>
- Khan, B. (2013). Functional near-infrared spectroscopy maps cortical plasticity underlying altered motor performance induced by transcranial direct current stimulation. *Journal of Biomedical Optics*, *18*, 116003. <https://doi.org/10.1117/1.jbo.18.11.116003>
- Lang, N., Siebner, H. R., Ward, N. S., Lee, L., Nitsche, M. A., Paulus, W., Rothwell, J. C., Lemon, R. N., & Frackowiak, R. S. (2005). How does transcranial DC stimulation of the primary motor cortex alter regional neuronal activity in the human brain? *European Journal of Neuroscience*, *22*, 495–504. <https://doi.org/10.1111/j.1460-9568.2005.04233.x>
- Liebetanz, D., Klinker, F., Hering, D., Koch, R., Nitsche, M. A., Pöschka, H., Löscher, W., Paulus, W., & Tergau, F. (2006). Anticonvulsant effects of transcranial direct-current stimulation (tDCS) in the rat cortical ramp model of focal epilepsy. *Epilepsia*, *47*, 1216–1224. <https://doi.org/10.1111/j.1528-1167.2006.00539>
- Liebetanz, D., Koch, R., Mayenfels, S., König, F., Paulus, W., & Nitsche, M. A. (2009). Safety limits of cathodal transcranial direct current stimulation in rats. *Clinical Neurophysiology*, *120*, 1161–1167. <https://doi.org/10.1016/j.clinph.2009.01.022>
- Lindenberg, R., Sieg, M. M., Meinzer, M., Nachtigall, L., & Flöel, A. (2016). Neural correlates of unihemispheric and bihemispheric motor cortex stimulation in healthy young adults. *Neuroimage*, *140*, 141–149. <https://doi.org/10.1016/j.neuroimage.2016.01.057>
- Ling, D., Rahman, A., Jackson, M., & Bikson, M. (2016). Animal studies in the field of transcranial electric stimulation. In A. Brunoni, M. Nitsche, & C. Loo (Eds.), *Transcranial direct current stimulation in neuropsychiatric disorders. Clinical principles and management* (pp. 67–83). Springer International Publishing. https://doi.org/10.1007/978-3-319-33967-2_5
- Merzagora, A. C., Foffani, G., Panyavin, I., Mordillo-Mateos, L., Aguilar, J., Onaral, B., & Oliviero, A. (2010). Prefrontal hemodynamic changes produced by anodal direct current stimulation. *Neuroimage*, *49*, 2304–2310. <https://doi.org/10.1016/j.neuroimage.2009.10.044>
- Mielke, D., Wrede, A., Schulz-Schaeffer, W., Taghizadeh-Waghefi, A., Nitsche, M. A., Rohde, V., & Liebetanz, D. (2013). Cathodal transcranial direct current stimulation induces regional, long-lasting reductions of cortical blood flow in rats. *Neurological Research*, *35*, 1029–1037. <https://doi.org/10.1179/1743132813Y.0000000248>

- Muthalib, M., Besson, P., Rothwell, J., & Perrey, S. (2018). Focal hemodynamic responses in the stimulated hemisphere during high-definition transcranial direct current stimulation. *Neuromodulation*, *21*, 348–354. <https://doi.org/10.1111/ner.12632>
- Nitsche, M. A., Fricke, K., Henschke, U., Schlitterlau, A., Liebetanz, D., Lang, N., Henning, S., Tergau, F., & Paulus, W. (2003). Pharmacological modulation of cortical excitability shifts induced by transcranial direct current stimulation in humans. *Journal of Physiology*, *553*, 293–301. <https://doi.org/10.1113/jphysiol.2003.049916>
- Nitsche, M. A., & Paulus, W. (2000). Excitability changes induced in the human motor cortex by weak transcranial direct current stimulation. *Journal of Physiology*, *527*, 633–639. [https://doi.org/10.1016/S0304-3940\(00\)01621-9](https://doi.org/10.1016/S0304-3940(00)01621-9)
- Nitsche, M. A., & Paulus, W. (2001). Sustained excitability elevations induced by transcranial DC motor cortex stimulation in humans. *Neurology*, *57*, 1899–1901. <https://doi.org/10.1212/WNL.57.10.1899>
- Paquette, C., Sidel, M., Radinska, B. A., Soucy, J.-P., & Thiel, A. (2011). Bilateral transcranial direct current stimulation modulates activation-induced regional blood flow changes during voluntary movement. *Journal of Cerebral Blood Flow and Metabolism*, *31*, 2086–2095. <https://doi.org/10.1038/jcbfm.2011.72>
- Paxinos, G., & Watson, W. (2005). *The rat brain in stereotaxic coordinates* (5th ed.). Elsevier Academic Press.
- Pellegrino, G., Maran, M., Turco, C., Weis, L., Di Pino, G., Piccione, F., & Arcara, G. (2018). Bilateral transcranial direct current stimulation reshapes resting-state brain networks: A magnetoencephalography assessment. *Neural Plasticity*, *2018*, 1–10. <https://doi.org/10.1155/2018/2782804>
- Peña-Gómez, C., Sala-Lonch, R., Junqué, C., Clemente, I. C., Vidal, D., Bargallo, N., Falcón, C., Valls-Solé, J., Pascual-Leone, Á., & Bartrés-Faz, D. (2012). Modulation of large-scale brain networks by transcranial direct current stimulation evidenced by resting-state functional MRI. *Brain Stimulation*, *5*, 252–263. <https://doi.org/10.1016/j.brs.2011.08.006>
- Pinheiro, J., Bates, D., DebRoy, S., Sarkar, D., & R Core Team. (2018). *nlme: Linear and nonlinear mixed effects models*. R package version 3.1-137. Retrieved from <https://CRAN.R-project.org/package=nlme>
- Polanía, R., Nitsche, M. A., & Paulus, W. (2011). Modulating functional connectivity patterns and topological functional organization of the human brain with transcranial direct current stimulation. *Human Brain Mapping*, *32*, 1236–1249. <https://doi.org/10.1002/hbm.21104>
- Polanía, R., Paulus, W., Antal, A., & Nitsche, M. A. (2011). Introducing graph theory to track for neuroplastic alterations in the resting human brain: A transcranial direct current stimulation study. *Neuroimage*, *54*, 2287–2296. <https://doi.org/10.1016/j.neuroimage.2010.09.085>
- Polanía, R., Paulus, W., & Nitsche, M. A. (2012). Reorganizing the intrinsic functional architecture of the human primary motor cortex during rest with non-invasive cortical stimulation. *PLoS ONE*, *7*, 30971. <https://doi.org/10.1371/journal.pone.0030971>
- R Core Team. (2014). *R: A language and environment for statistical computing*. R Foundation for Statistical Computing. Retrieved from <http://www.R-project.org/>
- Schmued, L. C., Stowers, C. C., Scallet, A. C., & Xu, L. (2005). Fluoro-Jade C results in ultra high resolution and contrast labeling of degenerating neurons. *Brain Research*, *1035*, 24–31. <https://doi.org/10.1016/j.brainres.2004.11.054>
- Sehm, B., Kipping, J., Schäfer, A., Villringer, A., & Ragert, P. (2013). A comparison between uni- and bilateral tDCS effects on functional connectivity of the human motor cortex. *Frontiers in Human Neuroscience*, *7*, 183. <https://doi.org/10.3389/fnhum.2013.00183>
- Sehm, B., Schaefer, A., Kipping, J., Margulies, D., Conde, V., Taubert, M., Villringer, A., & Ragert, P. (2012). Dynamic modulation of intrinsic functional connectivity by transcranial direct current stimulation. *Journal of Neurophysiology*, *108*, 3253–3263. <https://doi.org/10.1152/jn.00606.2012>
- Stagg, C. J., & Johansen-Berg, H. (2013). Studying the effects of transcranial direct-current stimulation in stroke recovery using magnetic resonance imaging. *Frontiers in Human Neuroscience*, *7*, 857. <https://doi.org/10.3389/fnhum.2013.00857>
- Stagg, C. J., & Nitsche, M. A. (2011). Physiological basis of transcranial direct current stimulation. *Neuroscientist*, *17*, 37–53. <https://doi.org/10.1177/1073858410386614>
- Takano, Y., Yokawa, T., Masuda, A., Niimi, J., Tanaka, S., & Hironaka, N. (2011). A rat model for measuring the effectiveness of transcranial direct current stimulation using fMRI. *Neuroscience Letters*, *491*, 40–43. <https://doi.org/10.1016/j.neulet.2011.01.004>
- Vines, B. W., Cerruti, C., & Schlaug, G. (2008). Dual-hemisphere tDCS facilitates greater improvements for healthy subjects' non-dominant hand compared to uni-hemisphere stimulation. *BMC Neuroscience*, *9*(1), 103. <https://doi.org/10.1186/1471-2202-9-103>
- Wachter, D., Wrede, A., Schulz-Schaeffer, W., Taghizadeh-Waghefi, A., Nitsche, M. A., Kutschenko, A., Rohde, V., & Liebetanz, D. (2011). Transcranial direct current stimulation induces polarity-specific changes of cortical blood perfusion in the rat. *Experimental Neurology*, *227*, 322–327. <https://doi.org/10.1016/j.expneurol.2010.12.005>
- Woods, A. J., Antal, A., Bikson, M., Boggio, P. S., Brunoni, A. R., Celnik, P., Cohen, L. G., Fregni, F., Herrmann, C. S., Kappenman, E. S., Knotkova, H., Liebetanz, D., Miniussi, C., Miranda, P. C., Paulus, W., Priori, A., Reato, D., Stagg, C., Wenderoth, N., & Nitsche, M. A. (2016). A technical guide to tDCS, and related non-invasive brain stimulation tools. *Clinical Neurophysiology*, *127*, 1031–1048. <https://doi.org/10.1016/j.clinph.2015.11.012>
- Zheng, X., Alsop, D. C. D., & Schlaug, G. (2011). Effects of transcranial direct current stimulation (tDCS) on human regional cerebral blood flow. *Neuroimage*, *58*, 617–632. <https://doi.org/10.1016/j.neuroimage.2011.06.018>

SUPPORTING INFORMATION

Additional supporting information may be found online in the Supporting Information section.

FIGURE S1 BOLD response to bilateral tDCS. BOLD signal time-courses in individual left and right sensorimotor and visual regions, on the cathodal and anodal stimulation sides, respectively, in response to bilateral tDCS. The modeled BOLD response is overlaid on each graph as a black line. M1, primary motor cortex; M2, secondary motor cortex; S2, secondary somatosensory cortex; S1FL, fore-limb region of the primary somatosensory cortex; S1HL, hind-limb region of the somatosensory cortex; V2, secondary visual cortex

FIGURE S2 BOLD signal in the visual cortex in response to bilateral tDCS over the sensorimotor cortex. BOLD signal time-courses in the visual cortex (V1 + V2) on the side of cathodal (left) and anodal (right) stimulation respectively, in response to bilateral tDCS of the sensorimotor cortex. The modeled BOLD response is overlaid on each graph as a black line. V1, primary visual cortex; V2, secondary visual cortex

FIGURE S3 Physiological parameters during simultaneous tDCS and fMRI. Physiological parameter values (mean (blue line) \pm SD (gray shading), $n = 5$) during the first fMRI session during which tDCS was

switched on (left panel), and for the second fMRI session during which tDCS was switched off (right panel). Recordings were occasionally affected by measurement drift, but levels remained within normal ranges. Data from one animal was excluded due to incomplete recording of peripheral capillary oxygen saturation and heart rate

FIGURE S4 Relative CBF change after bilateral tDCS. CBF changes after the first and second stimulation session (sham or tDCS) in the visual cortex (V1 + V2) and in individual left (cathodal side) and right (anodal side) sensorimotor and visual regions. Colored dots represent individual data-points. CBF, cerebral blood flow; L, left; M1, primary motor cortex; M2, secondary motor cortex; R, right; S2, secondary somatosensory cortex; S1FL, fore-limb region of the primary somatosensory cortex; S1HL, hind-limb region of the somatosensory cortex; V1, primary visual cortex; V2, secondary visual cortex

FIGURE S5 Changes in inter- and intrahemispheric functional connectivity following bilateral tDCS. (a) Change in intrahemispheric (left and right) and (b) interhemispheric functional connectivity

($\Delta(\text{Fisher's } z')$) between regions of interest within the sensorimotor and visual cortices, following stimulation (tDCS or sham stimulation) session 1 and 2. Colored dots represent individual data points. L, left; M1, primary motor cortex; M2, secondary motor cortex; R, right; S2, secondary somatosensory cortex; S1FL, fore-limb region of the primary somatosensory cortex; S1HL, hind-limb region of the somatosensory cortex; V1, primary visual cortex; V2, secondary visual cortex

Transparent Peer Review Report

Transparent Science Questionnaire for Authors

How to cite this article: Boonzaier J, Straathof M, Ardesch DJ, et al. Activation response and functional connectivity change in rat cortex after bilateral transcranial direct current stimulation—An exploratory study. *J Neurosci Res.* 2021;99:1377–1389. <https://doi.org/10.1002/jnr.24793>